Pablo Serra-Crespo[1,2,*]

Tim A. Wezendonk[1,*]

Carlos Bach-Samario[1]

Nishanth Sundar[1]

Karlijn Verouden[1]

Matthijs Zweemer[1]

Jorge Gascon[1]

Henk van den Berg[3]

Freek Kapteijn[1]

[1]Catalysis Engineering – ChemE, Delft University of Technology, Delft, The Netherlands.

[2]Radiation and Isotopes for Health – RST, Delft University of Technology, Delft, The Netherlands.

[3]Faculty of Science and Technology, Process Plant Design, University of Twente, Enschede, The Netherlands.

Preliminary Design of a Vacuum Pressure Swing Adsorption Process for Natural Gas Upgrading Based on Amino-Functionalized MIL-53

A preliminary study based on a conceptual process design methodology that includes a technical evaluation and an economic study has been carried out for the use of the metal-organic framework NH_2-MIL-53(Al) as adsorbent for the separation of carbon dioxide from methane. Among the alternatives considered, a vacuum pressure swing adsorption was chosen in the detailed design phase. The combination of a design with columns in parallel and the possibility of recirculating some of the streams ensures a high degree of separation and a final product with high quality without compromising the operation costs. A comparison with the state-of-the-art technology, amine scrubbing, and with a process based on membranes demonstrates that the proposed process is competitive as a result of its low operation costs and the energy demand.

Keywords: CO_2/CH_4 separation, Gas separation, Metal-organic framework, Natural gas upgrading, Pressure swing adsorption

1 Introduction

The demand for fossil fuels is predicted to continue increasing during the next few decades. Despite the fact that the available resources present higher concentration of impurities or undesired contaminants, the continuous increase in price is leading petrochemical companies to utilize reservoirs not previously considered. In case of natural gas exploitation, many sources contain up to 50 % of carbon dioxide (CO_2) [1]. Especially in these cases, purification of methane is needed, independently of its final use either as combustible or as raw material [2].

With the current technology, the most effective method of CO_2 capture is chemical absorption in an aqueous solution of an amine-based organic, such as mono- or diethanolamine (MEA, DEA) [3]. In the absorber, the gas is countercurrently "scrubbed" with an amine solution, typically capturing 85 % to 90 % of the CO_2. The solvent rich in CO_2 is then pumped to a second vessel (stripper), where heat is supplied in the form of steam to release the CO_2. The regeneration requires considerable energy, as not only the captured CO_2 has to be released at

higher temperatures, but also the evaporation losses of water are considerable [4].

Other technologies have been proposed for the removal of CO_2. Membrane-based separation has already been applied [5], demonstrating that it is possible to develop less energy-intensive separation schemes. Current drawbacks of membranes mostly lie in the necessity of pretreatments to remove any chemically reactive components and in the durability of the applied polymeric membranes [6]. Cryogenic distillation and microbial and algae systems have been proposed as well. Nonetheless, due to the high energy costs in the first case or because of the immature technology in the second, none of them has been applied in a large-scale industrial process [7, 8].

In view of the maturity of the technology and the development of highly selective adsorbents, the use of porous solids as adsorbents seems to be the technology with more opportunities to replace liquid-phase absorption as main technique for CO_2 removal on a short-term basis. Materials like activated carbons, silica gels, and zeolites have been widely proposed for this purpose [9, 10]. The major adsorptive separation technique that utilizes porous adsorbents is pressure swing adsorption (PSA). PSA is a cyclic process, consisting in most cases of several columns that are alternated in different steps. First, certain components of the gas mixture are selectively adsorbed on the adsorbent at a relatively high pressure, resulting in a gas stream that is richer in the less strongly adsorbed component of the gas fed. Once the packed porous material is saturated, the adsorbed components are desorbed by decreasing the pressure

Correspondence: Dr. Pablo Serra-Crespo (P.SerraCrespo@tudelft.nl), Prof. Freek Kapteijn (F.Kapteijn@tudelft.nl), Catalysis Engineering – ChemE, Delft University of Technology, Julianalaan 136, 2628 BL Delft, The Netherlands.

*These authors contributed equally.

in the column to near ambient pressure or even to sub-atmospheric pressures in the case of vacuum-swing adsorption. After this step, the adsorbent is regenerated and ready to be reused. The desorbed gases are enriched in the more strongly adsorbed component.

The main advantage of PSA is its low energy consumption and the easy regeneration of the adsorbent in most cases. PSA processes are a standard in the oil and gas industry, e.g., there are systems to purify hydrogen that may have up to 12 columns with cycles consisting of 20–30 steps and have been running for years. However, before PSA technology can be successfully applied in the separation of CO_2 from natural gas, adsorbents with higher capacities, higher selectivities, and easier regeneration need to be developed [11–15]. Metal-organic frameworks (MOFs) have been considered in the last decade as excellent candidates to overcome the issues mentioned above [16]. MOFs are crystalline compounds consisting of infinite lattices built up of the inorganic secondary building unit (SBU, metal ions or clusters) and organic linkers, connected by coordination bonds of moderate strength [17]. Distinct from traditional inorganic materials, MOFs can be synthesized from well-defined molecular building blocks thanks to both the reliability of molecular synthesis and the hierarchical organization via crystal engineering. MOFs can therefore be understood as molecules arranged in a crystalline lattice [18]. Even within such a relative short time span, the field has rapidly evolved from an early stage, mostly focused on the discovery of new structures, to a more mature phase in which several applications are being explored [19–22].

Many MOFs have been already reported as excellent candidates for the separation of CO_2, showing very good selectivities and high capacities [22–29]. One outstanding example is the amine-functionalized MIL-53. The terephthalate-based MOF MIL-53 is formed by metal-oxygen-metal chains that are interconnected by terephthalates resulting in 1D channels with diamond shape. The material exhibits a pore contraction or expansion upon the adsorption of certain molecules, such as CO_2, which is referred to in literature as the breathing effect [30, 31]. The breathing effect (see Fig. 1) has a beneficial influence on the separation of CO_2 from methane. When the material is in the so-called narrow-pore configuration, the adsorption of methane is hampered and decent selectivities are reached [32, 33]. Ferreira et al. have reported a combined experimental and design study in which they propose MIL-53(Al) as adsorbent for methane purification by applying vacuum PSA (VPSA) technology [34]. This is a good example of the type of studies that are needed before MOFs can be considered for their application in an industrial process.

The incorporation of an amine in the terephthalate modifies the breathing effect, the interaction of the amine with the bridging hydroxyl present in the metal-oxygen-metal chain
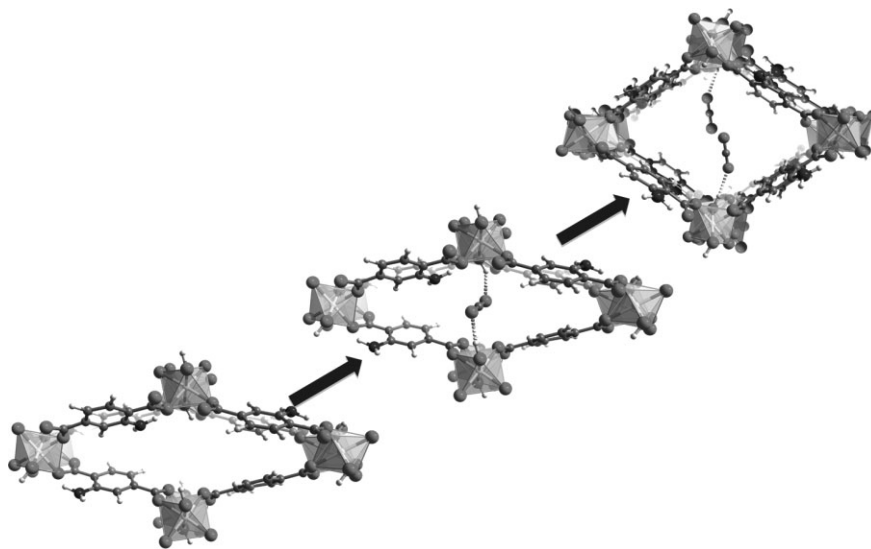

Figure 1. Schematic representation of the breathing effect in NH_2-MIL-53(Al) upon the adsorption of CO_2.

leads to the presence of the narrow-pore phase in the absence of adsorbate, and to a wider pressure range where this phase is dominant [35]. As a result of these two facts, NH_2-MIL-53(Al) exhibits one of the highest selectivities towards CO_2 reported in the MOF field [36].

In this contribution, a preliminary and simplified process design for the capture of CO_2 from natural gas based on the use of NH_2-MIL-53(Al) as adsorbent is presented. Technical and economic feasibility aspects are addressed with the intrinsic limitations of the many assumptions that were taken. Subsequently, a comparison with current industrial standards is performed, demonstrating the large potential of NH_2-MIL-53(Al) as selective adsorbent for natural gas sweetening. It is important to notice that the aim of this article is not to report a detailed and exhaustive design of an industrial process, but to show by means of a simplified approach the potential of NH_2-MIL-53(Al) as adsorbent for natural gas upgrading and to stimulate detailed studies, like the above-mentioned by Ferreira et al. [34], that bring the application of MOFs in industrial processes closer.

2 Design Methodology

A structural design method was applied to develop the process flow sheet for the required separation. The approach followed is shown in Fig. 2 [37, 38]. For the overall process, data about raw materials, battery limit processes, and CO_2 content were obtained from existing natural gas or oil wells, and provided a satisfactory basis of design [39–44]. For the separation, relevant information on adsorption, desorption, and operation conditions was obtained from laboratory data and from previously published contributions [36, 45–47]. This information provided input for the drafting of many design alternatives in the process synthesis that were assessed based on mass and heat balances calculations, which were translated into a process simulation model. The selection of the best case to further develop into a
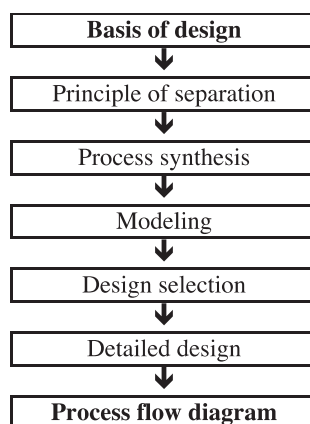
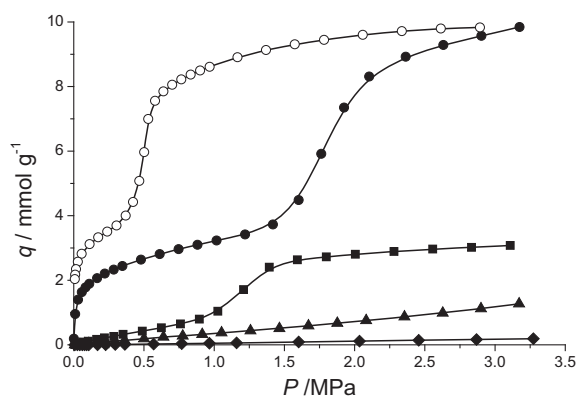Figure 2. Approach followed to develop the process flow diagram.

Figure 3. Adsorption isotherms at 298 K of (●) CO_2 (solid symbols for adsorption and open symbols for desorption), (■) methane, (▲) nitrogen, and (◆) hydrogen.

detailed design was based on rejection of the less attractive alternatives [48]. Finally, a detailed design including cycle times, process sizing, and implementation of control systems was carried out to obtain a process flow diagram of the conceptual design.

3   Principle of Separation

During the last few years, we have studied in detail and demonstrated the high application potential of NH_2-MIL-53(Al) in the separation of CO_2 [36, 45, 47, 49]. Despite the fact that it contains amine groups that could in principle interact with CO_2 in a similar fashion as liquid alcoholic amines do, no chemical interaction between amines and CO_2 was observed. The lack of interaction between the amines and CO_2 results in a relatively low heat of adsorption that allows an easy regeneration of the adsorbent without the need of increasing the temperature. That is in clear contrast with other conventional adsorbents like zeolites which are penalized by the need of heat and low pressure for their regeneration [35, 50, 51]. In addition, the material has shown long-term stability in the separation conditions and a high pressure resistance that would allow its manufacture and shaping [52, 53].

Single gas adsorption isotherms already indicate that CO_2 is preferentially adsorbed on NH_2-MIL-53(Al) over other gases like methane, nitrogen, and hydrogen; see Fig. 3. The plateau observed in the stepwise adsorption of CO_2 is related with the transition from the narrow-pore to the large-pore structure what provokes an increase in the maximum capacity of the material. The hysteresis loop that can be observed in the adsorption-desorption of CO_2 is due to the phase transition that occurs during the breathing effect and would imply the need of reaching a low partial pressure of CO_2 in a PSA system to obtain a high degree of regeneration.

Breakthrough experiments were carried out with a packed-bed column loaded with self-sustained pellets sieved between 500 and 710 μm. Prior to the experiment, the column was regenerated with a flow of helium. After the regeneration step, an equimolar mixture of CO_2 and methane was fed to the column. The mixture contained a low concentration of hydrogen

which is used as tracer assuming that it is not adsorbed. The flow out of the column was monitored continuously by a mass spectrometer. In Fig. 4, a breakthrough experiment at 298 K and a total pressure of 1 bar is presented for an equimolar mixture of CO_2 and CH_4.
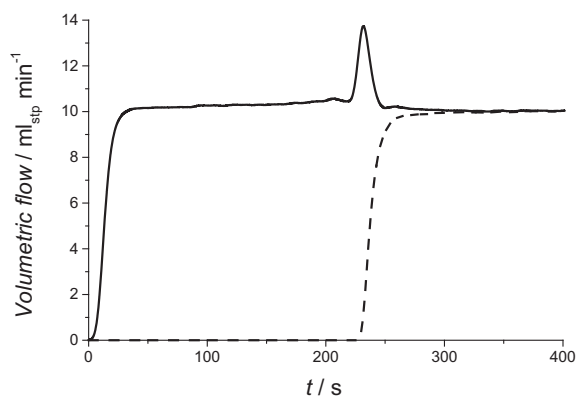

Figure 4. Breakthrough profiles at 298 K at a total pressure of 1 bar. Equimolar mixture of methane (full line) and CO_2 (dashed line).

The short delay between the breakthrough time of methane and time zero indicates the adsorption of a small amount of this compound. During a time period of around 230 s, only methane leaves the column and CO_2 is kept adsorbed in the porous material. Once the adsorbent is saturated, CO_2 is detected at the exit of the column. The peak observed in the methane profile at the time that CO_2 breaks through is caused by two factors: (i) a material with high selectivity and (ii) a post-column volume. More information about this phenomenon can be found elsewhere [47]. Both breakthrough profiles show a steep increase indicating the absence of strong diffusional limitations. After both gases are in equilibrium with the adsorbent, desorption is studied by changing to a pure helium stream. Desorption profiles can be found in Fig. 5. Within a few seconds, methane is completely desorbed, confirming its very low affinity for the adsorbent [47]. In case of CO_2, due to the much larger adsorption capacity, desorption takes longer.
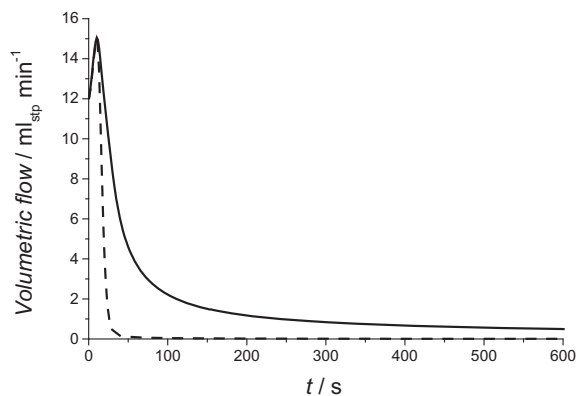
Figure 5. Breakthrough desorption profiles at 298 K at a total pressure of 1 bar. Equimolar mixture of methane (full line) and CO_2 (dashed line) purged with pure helium.

However, it should be stressed that full regeneration of the column takes place at room temperature and in a time frame similar to that of the adsorption cycle.

The readers are addressed to our recent contribution, an exhaustive study of breakthrough experiments that combines experimental and modeling approach for detailed information on the breakthrough interpretation. Information about mass balances, concentration and temperature profiles, and parameter estimation can be found there [47]. Data obtained at lab-scale (see Figs. 4 and 5) were used to calculate adsorption capacity and selectivity implemented in the later design of the process.

4 Process Synthesis

4.1 Methodology and Applied Process Synthesis

A systematic design procedure was applied following the methodology reported by Seider et al. to produce various design alternatives for the MOF-based separation process [38]. The methodology based on process synthesis principles is a way to define the approach of the design process. The process is drawn with sources and sinks in order to set the scope and battery limit of the project. For this process overview, data on raw materials and products are given in Tab. 1.

Many process schemes were devised and further developed towards preliminary process flow sheets. The selection of alternatives to develop in detail was based on the methods developed by Douglas, where the focus is put on the rejection of less attractive alternatives [48]. This multistep conceptual design method is described in more detail in the publications by Douglas [54] and by Seader and Westerberg [55].

4.2 Basis of Design and Selection of Design Alternatives

The process works on the basis of adsorption and regeneration. In the adsorption step, the feed gas flows through the packed bed where CO_2 is adsorbed. When the bed is fully loaded, the feed stream is switched to another unit and the bed is regener-

Table 1. Inputs for process synthesis.

Parameter	Value
Flow [MMscfd]	35
Inlet pressure [bar]	44.4
Inlet CH_4 mole fraction [–]	0.52
Inlet temperature [K]	298
Inlet CO_2 mole fraction [–]	0.48
CO_2 uptake at 1 bar [mol kg^{-1}]	2.0
CO_2 uptake at 35 bar [mol kg^{-1}]	8.0
CH_4 uptake at 1 bar [mol kg^{-1}]	0.2
CH_4 uptake at 40 bar [mol kg^{-1}]	0.8
MOF density [kg m^{-3}]	1750
Void fraction [–]	0.4

ated, either by changing pressure or temperature. In the basis of design, the selection was made to develop a PSA process selected among various alternatives of design. Furthermore, the application of heating in the regeneration step is discarded. The lab-scale experiments show that adsorbent regeneration can take place at the adsorption temperature due to the lack of chemical interaction between the adsorbates and the adsorbent, implying a relatively low heat of adsorption. For the sake of simplicity the process has been considered isothermal. This simplification is far from real conditions; in PSA systems differences of 40–50 °C can be easily found. In order to correct for such a deviation from the real behavior, the adsorbent capacity has been considered as 20 % lower, and accounting for an oversize in the column and the amount of adsorbent needed. The general operation steps of a PSA system are described thoroughly in the section detailed design.

Various functional process schemes were produced and assessed. Preliminary mass balances incorporating physical properties, laboratory data, and process conditions provided a first insight in the efficiency and capacity of such systems. The analysis indicated that an important parameter in the design costs is the adsorption pressure of the column. As found in the NH_2-MIL-53(Al) isotherm data, it is evident that at pressures below 5 bar there is virtually no methane uptake, and thus the separation factor is very high [56]. However, the capacity of CO_2 is nearly four times as low, i.e., 2 mol kg^{-1} versus 8 mol kg^{-1}. This is reflected in both the adsorbent investment costs, i.e., the costs of the amount adsorbent needed to process the incoming natural gas stream at the battery limit, and the energy requirement of the process. Not only the adsorbent investment costs rise a fourfold, but the energy required to remove a molecule of CO_2 from the stream increases around 16 times. This increase is due to the requirement at the downstream battery limit of the process since a pressure over 40 bar is needed to transport and further process the natural gas stream. For all these reasons it is convenient that the operation pressure of the separation process is kept at the same value as the feed, being 44 bar, the chosen operation pressure.

Methane losses in the process can be a detrimental parameter if they are not properly addressed. Operation at elevated pressures will increase the uptake of methane but that can be minimized with the inclusion of a recycle stream that will improve the economic potential of the process.

Design alternatives that provided solutions to utilize the full capacity of the adsorbent are found to have a much higher economic potential, as can be easily understood in relation to the high adsorbent investment costs. After depressurization, a sufficient amount ($1\,mol\,kg^{-1}$) of CO_2 is still present on the adsorbent. If not desorbed and captured, the working capacity would decrease and the column would need an additional 12.5 % increase in capacity to compensate. Therefore, the application of vacuum (200 mbar) in the blow-down step is preferred, and the process can be considered more specifically a VPSA.

In total, seven alternatives were assessed based on mass and heat balances calculations. The selection of the alternative to be further developed into a detailed design was based on several rejection criteria such as methane product stream purity and methane loss of the process, and especially the total adsorbent costs of the process alternative. The costs of the adsorbent resulted to be a large part of the total expenditure, thus pointing to the importance of optimal usage of the adsorbent. Related to operation, the energy requirement of the process and utility capital costs were taken into account as criteria for selection. More information about the different studied alternatives and the selection criteria can be found elsewhere [57].

In the selected alternative, natural gas is brought into a PSA separation column, which is operated at 44 bar with a recirculation depending on the operational step. By switching between operational modes, pure methane and CO_2 are obtained at the outlet without losing valuable methane. The alternative includes the evacuation of the vessel after the depressurization phase, in contrast to experiments in lab-scale where helium was used to regenerate the column. Note that continuous operation can only be carried out by utilizing more than one separation column.

The above-mentioned alternative is selected for detailed design and further analysis. Its main advantage is the reduced energy consumption compared to other alternatives. Due to the complexity of the process and for the sake of simplification, the assumption of an isothermal process was taken and the number of columns is reduced to two. To compensate for the decrease in capacity due to an increase in temperature, the saturation capacity of the adsorbent has been considered as $8\,mol\,kg^{-1}$, a 20 % lower than observed experimentally. Typically, a larger number of columns is considered for PSA systems; however, the scope of this contribution is to show the potential of an adsorption process based on NH_2-MIL-53(Al) and not to give a detailed and complete process design.

5 Process Design

The goal of the process design is to obtain insight into the total process inventory to support the process evaluation by data. With all equipment listed and the separate units properly designed, the operation can be visualized and a complete process flow diagram can be drafted. A comprehensive description of the VPSA process, which is based on the design proposed by Guerin de Montgareuil and Domine [58], is given next and a schematic view is found in Fig. 6 that includes the pressure variation in the different steps.
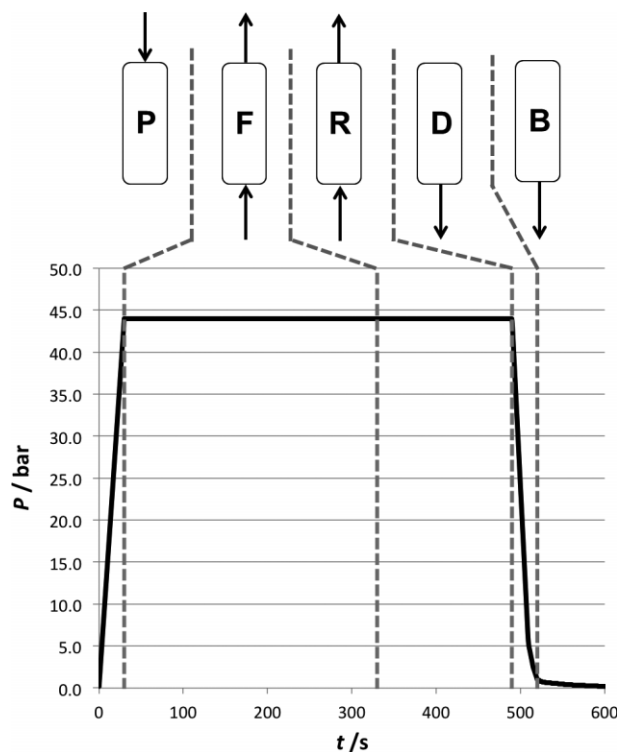

Figure 6. Different steps during a PSA cycle including their step times. (P) pressurization, (F) feed, (R) rinse, (D) depressurization, and (B) blow-down.

In the first step, there is a countercurrent pressurization in which methane from the product stream is utilized to increase the pressure in the column from vacuum at ~ 0.2 bar up to 44 bar. The pressurization step is followed by the feed. The mixture of CO_2 and methane at 44 bar is fed from the bottom combined with a recycle stream that comes from the other column which is in the rinse step. Purified methane leaves the top of the column and CO_2 is selectively adsorbed.

In the next step, known as rinse, a CO_2-enriched stream from the depressurization is fed from the bottom at 44 bar to rinse the system with a low flow rate of CO_2. In this step, the methane in the gas and adsorbed phase is displaced by CO_2 what leads to a higher yield and selectivity, as it was recently reported [56]. The resulting mixture of this step is supplied to the other column together with the feed.

Depressurization and blow-down of the column take place after the rinse. In depressurization, the saturated column releases its pressure bottom-down and the whole gas phase is evacuated together with part of the adsorbed CO_2. Part of the depressurization stream is stored in a temporary storage vessel and it will be utilized, after repressurization, in the rinse step. Once atmospheric pressure is reached, an inline vacuum pump is used in the blow-down step to decrease the pressure to

0.2 bar and help desorbing the CO_2 remaining in the adsorbent that is conducted to a storage vessel or to a transport line. After this step the cycle starts again with the pressurization

The feed stream entering the separation unit has a fixed flow rate, based on the 35 MMscfd (SS 310 kg h^{-1}) of natural gas that should be handled by the process (see Tab. 1); this value was selected according to production of similar plants [6]. The final composition of the feed has been selected among different alternatives, finally the composition based on the Kapuni field was chosen because of the high concentration of CO_2 and the absence of hydrogen sulfide [59, 60]. A similar composition has been chosen by Ferreira et al. in their evaluation of the unfunctionalized MIL-53(Al) as adsorbent for methane purification [34].

The different cycle times are based on the experimental data and industrial standards of PSA technologies found in different literature sources [58, 61, 62]. Cycle times in conventional PSA systems are in the order of 10 min [63]. The stage that will require most of the cycle time is the feed step which is considered to take 5 min for columns under similar conditions [64]. With the flow rate, the adsorbent capacity, and adsorption time set, the column can be sized. The time for the rinse was adjusted according to the residence time that the CO_2 stream needs to reach the outlet of the bed. The depressurization and repressurization phases of the cycle are set according to the time required for such operations in industrial PSA and for an efficient application of the utility units, such as compressors and vacuum pump [63]. In the depressurization phase, the evacuation of the column is coupled to obtain a single cycle time description. Similar time distribution in the different cycle steps can be found in many studies with comparable systems [65–68].

The cycle time analysis revealed that, already with two columns in parallel, pseudo-continuous operation could be achieved; see Fig. 7 and Tab. 2. The main advantage of the high occupancy of the adsorbent is the limited number of columns that are loaded with this adsorbent. In contrast, the disadvantage is the extra process inventory related to the pressurization step that is now utilizing part of the enriched methane gas to pressurize the column prior to switching to the feed stream. By including that in the PSA column, the compound adsorbed will be distributed in an initial zone where equilibrium is achieved, and into a mass transfer zone close to the other end of the col-

Table 2. Cycle times in the VPSA system.

	Cycle time [s]
Repressurization	30
Adsorption	300
Rinse	160
Depressurization	30
Blow-down	80

umn where the adsorbent is not completely saturated. Therefore, it is assumed that high-purity methane exiting is maintained during adsorption. Mass flows of the different currents in the process with their molar fractions are given in Tab. 3.

Table 3. Mass flow of the different currents in the process with their correspondent molar fractions.

	Mass flow [kg h^{-1}]	Molar fraction [–]
Feed	55 310	0.518
Recycle	3612	0.829
CH$_4$ product	18 060	1
CO$_2$ product	37 250	0

Based on these conditions, the columns and utility equipment were designed. One of the critical factors in the design of the adsorption column is the pressure drop that will mainly depend on the pellet size together with the L/D ratio. In this way, it is closely related to the bed performance, as the overall mass transfer rate of CO_2 in the bed is affected by external transport from the gas to the adsorbent particle surface, axial dispersion and gas phase back mixing, and internal transport within the adsorbent pellets.

The particle size and vessel sizing have the greatest influence on the pressure drop. To relate to similar industrial systems, pellet sizes of zeolite used in CO_2 removal in PSA systems were examined [69]. As NH$_2$-MIL-53(Al) has shown very little kinetic limitations on the crystal and pellet scale [45, 56, 70], it
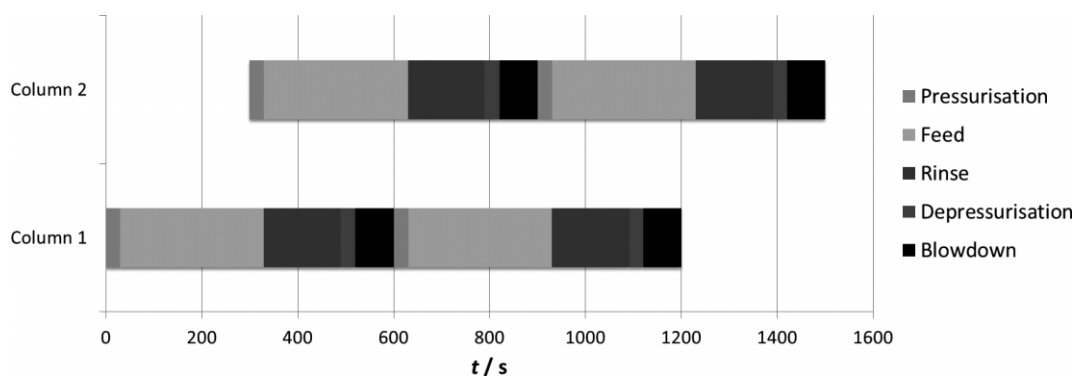

Figure 7. Cycle times in the proposed VPSA system that includes two parallel columns.

is assumed that using cylindrical pellets with 3 mm diameter would not exhibit mass transport limitations. The pellet is assumed to be a perfect cylinder with a height that equals the diameter. Each column is loaded with 7570 kg of adsorbent, which is the amount needed to process the feed in the calculated cycle time.

The pressure drop was calculated by the Ergun equation [71, 72]. The effect of the length over diameter (L/D) ratio was analyzed, as the performance of the PSA system is dependent on the mass transfer zone that stretches over the length of the bed. The optimum for the pressure drop value was determined by addressing as well the economy of scale of the vessel. Lists of "off-the-shelf" pressure vessels readily show certain L/D ratios for various fixed column volumes [73]. The final size of the columns is 7.6 m^3 in volume with a diameter of 1.1 m and a length of 8 m that results in a pressure drop of $\sim$ 2 bar. The size of the columns and the extra storage vessels can be found in Tab. 4.

Table 4. Size details of the different vessels in the process.

Equipment	Volume [m^3]	Diameter [m]	Length [m]
Column (two pieces)	7.6	1.1	8
Storage tank I	10	1.2	8.9
Storage tank II	40	1.85	14.9
Storage tank III	400	7.5	9

Besides the two separation columns, there are three storage tanks required for the intermediate storage of methane (II), CO_2 (III), and the recycle stream (I). Furthermore, three compressors and one vacuum pump need to be installed to attain an operation as designed. Their specifications are listed in

Tab. 5. The pump and compressor ratings have been calculated based on the cycle times and process flows. The storage vessels followed design procedures similar to the adsorption column. All process units added to the process together with the results from the mass balance are presented in Fig. 8.

Table 5. Capacity and power of the different compressors and vacuum pump.

Equipment	Type	Capacity [m^{3}s^{-1}]	Power [kW]	Suction/ discharge pressure [bar]
Compressor I	Centrifugal	0.023	9.1	35.2/44.4
Compressor II	Centrifugal	0.600	245	37.7/44.4
Compressor III	Centrifugal	1.350	925	1/44.4
Vacuum pump	Blower	5.360	805	0.1/1

6 Economic Evaluation

The economic potential (EP$_0$) of the process together with the capital cost expenditure have been estimated by a financial analysis. The economic potential is calculated at the initial state of the project and serves as an order-of-magnitude estimate. The preliminary and full estimates are based on available pricing and correlations, and use rules of thumb to obtain a more rigid cost estimate.

The order-of-magnitude estimate is based on the raw material and product specification, plant capacity, and utility requirements. The study estimate takes into account more variables such as location, PFDs, equipment lists, approximate size of structures, utility quantities, and piping and engineering costs.
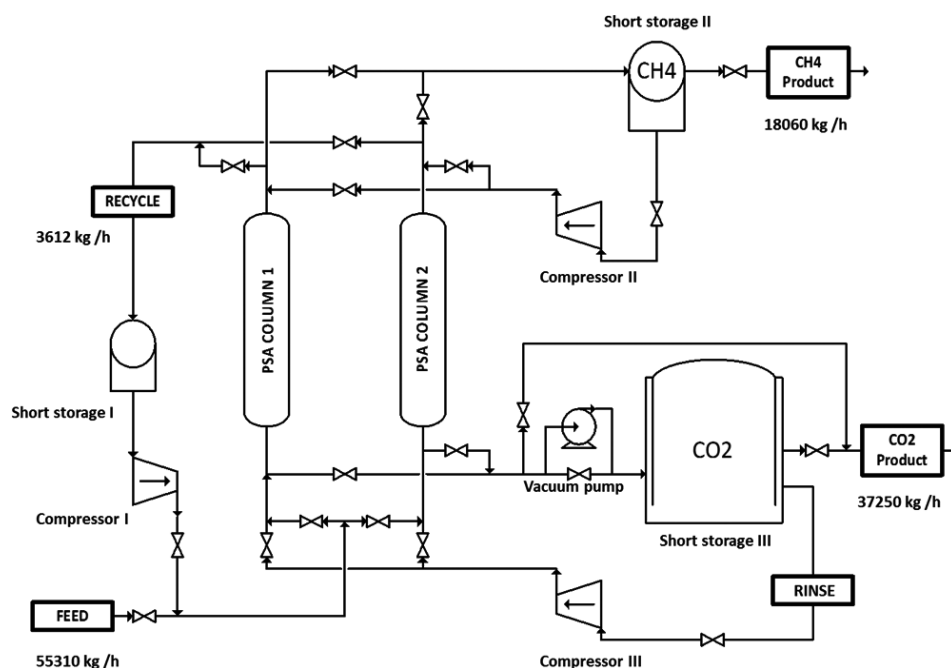

Figure 8. Process flow diagram of the VPSA based on NH$_2$-MIL-53(Al) including the most important mass flows in the process.

This evaluation gives a first insight into the feasibility of the process. The EP_0 is thus defined as the economic potential of the products minus the raw materials. It is obtained in the pre-design stage by relating the sources and sinks with their corresponding values. In order to obtain these values for the products and raw materials, a value chain analysis was carried out over the natural gas chain. The value for the gross production of natural gas after separation and purification is determined at $0.12 \in m^{-3}$. The raw material price depends on the supplier, demand, and composition, however, a price of $0.02 \in m^{-3}$ is a fair estimation. The pretreatment is then assumed to double the price of the natural gas to $0.04 \in m^{-3}$ [74, 75]. Costs of CO_2 emissions were not considered. These values result in an economic potential of 16 M€ per year within the planned capacity. A sensitivity analysis for the natural gas market was carried out as well. The economic potential set the maximum capital investment at 100 M€ with a payback time of ten years.

The evaluation of changing market conditions has been performed by means of a sensitivity analysis. The price of the natural gas limits the feasibility of the separation process. The price of the natural gas that makes the cash flow become negative is around $0.06 \in m^{-3}$.

The capital expenditure of the plant was calculated to determine the total investment needed for the project realization. The economic potential (EP_0) and internal rate of return (IRR) are required parameters for the calculation of the CapEx. EP_0 has been determined by relating the sources and sinks, which results in a value of 16 M€ per year. The IRR is given and fixed at 10 %. By varying the payback time (PBT) from five to ten years, the calculated maximum capital expenditure ranges from 60 to 100 M€, respectively, which are the boundaries of the project.

The economic potential is mostly a predesign analysis to determine the maximum capital investment and to analyze the feasibility. Therefore, the EP_0 is followed by a study estimate. The study estimate is based on the Factor Method developed by Lang [38] and consists of direct and indirect costs. The indirect costs are related to project services such as engineering and administration, and direct costs involve construction costs from equipment like property, vessels, utilities, and other materials. The direct costs can be obtained directly from the processes. The piping, buildings, and other auxiliaries have been calculated by the Lang factors (f). Indirect costs are often estimated by the use of ratios over the total direct plant costs, i.e.,

the Lang factors. The costs for land, start-up, and working capital have been estimated over the total depreciable capital and total permanent investment. The total capital investment has been calculated as a sum of the separate stages. A breakdown of these cost stages is given in Tab. 6.

The value for the purchased equipment costs (PEC) is estimated using sources of equipment prices, methods of adjusting equipment prices for capacity and depreciation, and relating auxiliary equipment to the main process. The main source for the PEC is the equipment inventory, which provides the properties of the utilities. The estimates were carried out with the help of the DACE handbook [76], the capital costs chapter of Seider et al. [38] and the cost estimation, design and equipment chapters of Peters et al. [77].

The equipment prices were found by directly selecting the required values from the DACE handbook or selecting the values from figures in Seider et al. [38, 73]. It was necessary to estimate the cost of equipment when data were unavailable for the particular size and operation. Seider et al. and Peters et al. provided the economy of scale correlations and the corresponding exponentials factors. The exponential value can be defined as 0.6, which is referred to as the six-tenth rule [38, 77].

The value for the total capital investment (TCI) is derived from the PEC taking into account the Lang factors for the different stages. The Lang factors f_1, f_2, f_3, f_4, and f_5 are taken from Peters et al., being 3.5, 0.21, 0.15, 0.06, and 0.08, respectively [77]. All the factors are based on a battery limit installation in a fluid-processing process, as only gaseous compounds are processed on-site.

An important part of the invested capital is the price of the adsorbent. The estimation of the costs per mass of this NH_2-MIL-53(Al) adsorbent based on costs at lab-scale gives a price of around $410 \in kg^{-1}$. The already reported values for the starting materials to produce MOFs from similar precursors were found to be much lower compared to the number utilized for the design of this process [78]. Furthermore, the amount of adsorbent needed was overestimated by 20 % to compensate the simplification that considers the process to be isothermal. In total, for the amount of adsorbent needed to load both columns, the estimate capital investment is 6.21 M€ based on the 7570 kg needed for each column.

It is important to note that because of the enormous value for the adsorbent capital, the adsorbent costs were not included in the PEC calculation, but simply added to the total direct

Table 6. Breakdown of the Lang factor method for the study estimate.

Stage	Calculation	Stage buildup	[M€]
Purchased equipment costs (PEC)	PFD, P&ID. Pricing; Peters and Timmerhaus, DACE Handbook	Costs of separation vessels, compressors, vacuum pump, intercoolers, storage vessels	2.66
Total direct plant costs (TDPC)	PEC + $f_1 \times$PEC	Installation, instrumentation and control, piping, electrical, buildings, services, yard improvements, adsorbent costs	18.18
Total plant costs (TPC)	TDPC + $f_2 \times$TDPC	Engineering and supervision, construction expenses	21.99
Total depreciable capital (TDC)	TPC + $f_3 \times$TPC	Contractor's fee, legal expenses, contingency	25.30
Total permanent investment (TPI)	TDC + $f_4 \times$TDC	Start-up, spares, storage, royalties or patents	26.82
Total capital investment (TCI)	TPI + $f_5 \times$TPI	Working capital	28.96

plant costs (TDPC). This assumption is a result of the inconsistently high PEC, which accumulates through the TCI calculation. As a result of this consideration, the total capital investment or capital expenditure (CapEx) is 29 M€.

If the adsorbent price is higher, the CapEx will rise significantly. In turn, if an industrial process able to manufacture a much cheaper adsorbent is developed, the CapEx will decrease with a large value. This situation is illustrated in Fig. 9, where the CapEx of the parallel process is given as a function of the adsorbent cost per kg. It is observed that the CapEx is reduced to the TCI price of equipment and utilities alone for adsorbent costs in the order of other adsorbents like zeolites with prices between 1 and 50 € kg^{-1}.
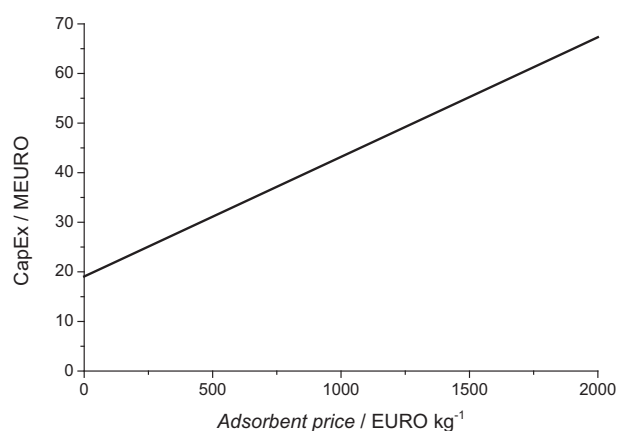

Figure 9. Capital expenditure (CapEx) as function of the adsorbent's price.

The next costs that need to be estimated are the production costs, based on the operating labor, utilities, maintenance, and repairs. These sections will be referred to as the operational expenditure (OpEx). The total OpEx for the parallel process is 1.8 M€ per year.

The study estimate was carried out to obtain a more accurate cost estimate of the designed process. It was based on available pricing and correlations of the process flow diagrams and piping and instrumentation diagrams. The capital expenditure was calculated as 29 M€ and the operational expenditure as almost 2 M€ per year.

The cost estimation for the CapEx and OpEx are both well below the maximum capital investment and cash flow from the economic potential. These values provide a feasible window to operate the designed alternative.

7 Process Evaluation

The studied VPSA option is based on the use of NH$_2$-MIL-53(Al) as adsorbent. This technology has not been applied in CO$_2$ separation processes, and, therefore, the outcomes of these processes should be evaluated. In this section, the proposed process is compared to the most widely applied CO$_2$ separation processes in industry to evaluate its potential. The factors that are compared to evaluate the process are mainly the capital

investment, the operating cost (OC), the operating expenses (OE), and the energy consumption. The difference between the OC and the OE is that the latter includes the expenses related to the methane losses.

Several cost estimations should be done to calculate the overall operating expenses. For the energy costs, the fraction of time has been taken for the equipment multiplied by the 8000 h of operation a year. The total uptime a year has been multiplied by the energy demand of the stated pump or compressor and multiplied by the energy costs of 0.10 € kWh^{-1}. The labor costs have been calculated using inflation ratios as well as the workload based on the throughput of a plant, i.e., 55 h d^{-1}. With a salary of 30 € h^{-1} the labor costs were obtained. Finally, the maintenance costs are considered which are based on a ratio of the total capital investment. For fully automated processes, this factor should be on the lower side between 0.02 and 0.06. For the parallel process it is chosen for 0.02 and the series process for 0.025 as both processes are fully automated and the series process is slightly more complicated. The labor and maintenance assumption are based on values according to Peters et al. [77]. Finally, an OE value of 1.83 M€ is obtained. Due to the low methane losses that are generated in the process, the same value would be found for the OC, but to obtain a more realistic approach, the values included in Tab. 7 cover the OC considering methane losses in the range of the compared technologies.

Table 7. Economical comparison between the studied processes.

	Membrane	Amine scrubbing	VPSA
Total capital investment, TCI [M€]	4.80	10.54	29
Methane losses, HL [M€ a^{-1}]	1.36	0.17	0.2–1.5
Operating expenses, OE [M€ a^{-1}]	1.75	4.83	1.8
Operating costs, OC [M€ a^{-1}]	3.11	5.00	2–3

Estimated accuracy ± 30 %.

Other comparisons among the different technologies have been reported before. One example is from Bhide et al., where a detailed cost estimation comparing amine scrubbing with a membrane process for the separation of CO$_2$ with a feed flow of 35 MMscfd was reported [6]. This study has been used for the comparison with the proposed VPSA process using NH$_2$-MIL-53(Al) as adsorbent.

The economic data reported in the publication were updated and the amount of CO$_2$ processed for both technologies increased and corrected to match the characteristics of the proposed VPSA system. Also some other considerations were taken into account to produce a much more fair comparison. The total capital investment of the amine scrubber and the membrane processes have been multiplied by the chemical engineering plant cost ratio as indicated by Peters et al. [77]. To compensate for the higher CO$_2$ content (from 0.25 to 0.44 on a molar basis), an extra ratio of 1.5 has been applied to the TCI. Methane value losses have been considered to increase from 2 to 3 $ MBtu^{-1} in accordance with methane actual prices. The operation expenses are related to the TCI by the Lang fac-

tors, and the operations costs are the combination of methane losses and operation expenses.

By comparing these figures (see Tab. 7), it can be derived that: (i) the TCI for the MOF-based project is much higher, mainly because of adsorbent price, (ii) the OE for the VPSA and the membrane process are similar and about one-third of the OE of the amine scrubbing process, (iii) the OC of the VPSA and membrane process are similar, while the OC for the amine scrubbing process is 50 % higher, and (iv) the costs for methane losses are most probably the lowest for the amine scrubbing process.

Even though the adsorbent cost is a crucial part of the total capital investment, this fact can be compensated by the lower operating costs on a long-term basis. If the adsorbent can be utilized during a long period of time, the process number would become more profitable than the other alternatives. When comparing the VPSA MOF-based system with the amine scrubbing process, a period of six years is needed for the proposed design to be competitive. If it is compared with membrane technology, 20 years are required. However, in none of the cases, the replacement of the absorbing solvent (continuous make-up) or of the membranes (about three years lifetime) are considered. This will decrease noticeably the economic gap between the VPSA system and the membrane process if the membrane substitution is included in the operating expenses because a long operation life is expected for NH_2-MIL-53(Al) according to the stable performance showed in lab-scale for years [6, 45].

If the energy consumption is evaluated in terms of MJ consumed per kmol of CO_2 separated, the current MEA processes need around $200\,MJ\,kmol^{-1}$ of CO_2 removed. However, the state-of-the-art CO_2 separation using methyldiethanolamine (MDEA) decreases the value to about $100\,MJ\,kmol^{-1}$ [79]. If the VPSA system is studied in this perspective and considering the energy demand from pumps and compressors, the energy demand in this process is around $10\,MJ\,kmol^{-1}$, a value ten times lower than the currently applied technology, and it does not make use of toxic and corrosive compounds. Even though that it is just a rough estimation, it already gives a clear indication of the low energy consumption of this process.

From the above evaluations, several important points can be emphasized. In the first place, the VPSA process does not employ any corrosive or toxic compounds that may affect the sorbent, and the lifetime of the adsorbent is expected to be much longer than the currently used membrane lifetime of three years. The total capital investment is rather high compared to the amine scrubber and membrane process, mainly due to the estimated price of the adsorbent, which is expected to be lower once an industrial process is developed for its synthesis. Furthermore, the operating costs of the VPSA processes are lower. Finally, the comparison of the energy consumption between VPSA and amine scrubbing shows that the VPSA processes are at least ten times less energy-consuming. These values do not represent real-life costs of the processes, but they provide insights into the relative costs and the feasibility of the process.

8   Conclusions

A vacuum pressure swing adsorption process, based on the utilization of the metal-organic framework NH_2-MIL-53(Al) for the separation of CO_2 from CH_4, has been proposed based on a conceptual process design analysis. The analysis includes a technical evaluation, an economic study, and a comparison with the most widely applied technologies.

In the early stage of the design analysis, several alternatives were considered by applying conceptual design methods, and the most appropriate passed a design phase. The use of columns in parallel at high pressure combined with a recycle stream assures a high amount of methane recovery.

In the detailed design phase, the selected design alternative was further developed including equipment and unit design, process control, safety and economical evaluation. From the obtained values it can be concluded that the designed process provides a high-quality product and can be operated in a cost-effective way. The comparison with the most applied technologies, namely, amine scrubbing and membrane-based processes, proves that the studied system is competitive due to its low operation costs and energy demand.

Despite the fact that this study is a preliminary study and many assumptions had to be taken like the adsorbent price and isothermal operation conditions, the figures point to a process with a substantial potential in this early design phase. We hope that the potential showed by this contribution boosts further studies that include a more exhaustive and realistic approximation and bring closer the incorporation of metal-organic frameworks as adsorbents in industrial processes.

Acknowledgment

The authors have declared no conflict of interest.

References

[1]   S. Sircar, *Sep. Sci. Technol.* **1988**, *23*, 519–529.

[2]   J. D. Figueroa, T. Fout, S. Plasynski, H. McIlvried, R. D. Srivastava, *Int. J. Greenhouse Gas Control* **2008**, *2*, 9–20.

[3]   P. V. Danckwerts, *Chem. Eng. Sci.* **1979**, *34*, 443–446.

[4]   A. B. Rao, E. S. Rubin, *Environ. Sci. Technol.* **2002**, *36*, 4467–4475.

[5]   E. Favre, *J. Membr. Sci.* **2007**, *294*, 50–59.

[6]   B. D. Bhide, A. Voskericyan, S. A. Stern, *J. Membr. Sci.* **1998**, *140*, 27–49.

[7]   A. Hart, N. Gnanendran, *Energy Procedia* **2009**, *1*, 697–706.

[8]   X. Wang, Y. Feng, J. Liu, H. Lee, C. Li, N. Li, N. Ren, *Biosens. Bioelectron.* **2010**, *25*, 2639–2643.

[9]   S. Choi, J. H. Drese, C. W. Jones, *ChemSusChem* **2009**, *2*, 796–854.

[10] M. Tagliabue, D. Farrusseng, S. Valencia, S. Aguado, U. Ravon, C. Rizzo, A. Corma, C. Mirodatos, *Chem. Eng. J.* **2009**, *155*, 553–566.

[11] S. Sircar, *Ind. Eng. Chem. Res.* **2002**, *41*, 1389–1392.

[12] A. M. Ribeiro, J. C. Santos, A. E. Rodrigues, S. Rifflart, *Sep. Sci. Technol.* **2011**, *47*, 850–866.

[13] A. M. Ribeiro, C. A. Grande, F. V. S. Lopes, J. M. Loureiro, A. E. Rodrigues, *Chem. Eng. Sci.* **2008**, *63*, 5258–5273.

[14] A. M. Ribeiro, J. C. Santos, A. E. Rodrigues, S. Rifflart, *Energy Fuels* **2012**, *26*, 1246–1253.

[15] A. Ribeiro, J. Santos, A. Rodrigues, *Adsorption* **2011**, *17*, 443–452.

[16] M. Gaab, N. Trukhan, S. Maurer, R. Gummaraju, U. Müller, *Microporous Mesoporous Mater.* **2012**, *157*, 131–136.

[17] H.-C. Zhou, J. R. Long, O. M. Yaghi, *Chem. Rev.* **2012**, *112*, 673–674.

[18] C. Wang, D. Liu, W. Lin, *J. Am. Chem. Soc.* **2013**, *135*, 13222–13234.

[19] J. Gascon, A. Corma, F. Kapteijn, F. X. Llabrés i Xamena, *ACS Catal.* **2014**, *4*, 361–378.

[20] R. J. Kuppler, D. J. Timmons, Q.-R. Fang, J.-R. Li, T. A. Makal, M. D. Young, D. Yuan, D. Zhao, W. Zhuang, H.-C. Zhou, *Coord. Chem. Rev.* **2009**, *253*, 3042–3066.

[21] J. Lee, O. K. Farha, J. Roberts, K. A. Scheidt, S. T. Nguyen, J. T. Hupp, *Chem. Soc. Rev.* **2009**, *38*, 1450–1459.

[22] J.-R. Li, R. J. Kuppler, H.-C. Zhou, *Chem. Soc. Rev.* **2009**, *38*, 1477–1504.

[23] K. Sumida, D. L. Rogow, J. A. Mason, T. M. McDonald, E. D. Bloch, Z. R. Herm, T.-H. Bae, J. R. Long, *Chem. Rev.* **2011**, *112*, 724–781.

[24] Y. Liu, Z. U. Wang, H.-C. Zhou, *Greenhouse Gases Sci. Technol.* **2012**, *2*, 239–259.

[25] S. Chaemchuen, N. A. Kabir, K. Zhou, F. Verpoort, *Chem. Soc. Rev.* **2013**, *42*, 9304–9332.

[26] J.-R. Li, Y. Ma, M. C. McCarthy, J. Sculley, J. Yu, H.-K. Jeong, P. B. Balbuena, H.-C. Zhou, *Coord. Chem. Rev.* **2011**, *255*, 1791–1823.

[27] S. D. Kenarsari, D. Yang, G. Jiang, S. Zhang, J. Wang, A. G. Russell, Q. Wei, M. Fan, *RSC Adv.* **2013**, *3*, 22739–22773.

[28] S. Keskin, T. M. van Heest, D. S. Sholl, *ChemSusChem* **2010**, *3*, 879–891.

[29] J.-R. Li, J. Sculley, H.-C. Zhou, *Chem. Rev.* **2011**, *112*, 869–932.

[30] F. Millange, C. Serre, G. Férey, *Chem. Commun.* **2002**, 822–823.

[31] C. Serre, F. Millange, C. Thouvenot, M. Nogues, G. Marsolier, D. Louer, G. Férey, *J. Am. Chem. Soc.* **2002**, *124*, 13519–13526.

[32] V. Finsy, L. Ma, L. Alaerts, D. E. De Vos, G. V. Baron, J. F. M. Denayer, *Microporous Mesoporous Mater.* **2009**, *120*, 221–227.

[33] L. Hamon, P. L. Llewellyn, T. Devic, A. Ghoufi, G. Clet, V. Guillerm, G. D. Pirngruber, G. Maurin, C. Serre, G. Driver, W. v. Beek, E. Jolimatre, A. Vimont, M. Daturi, G. Férey, *J. Am. Chem. Soc.* **2009**, *131*, 17490–17499.

[34] A. F. P. Ferreira, A. M. Ribeiro, S. Kulaç, A. E. Rodrigues, *Chem. Eng. Sci.* **2015**, *124*, 79–95.

[35] E. Stavitski, E. A. Pidko, S. Couck, T. Remy, E. J. M. Hensen, B. M. Weckhuysen, J. Denayer, J. Gascon, F. Kapteijn, *Langmuir* **2011**, *27*, 3970–3976.

[36] S. Couck, J. F. M. Denayer, G. V. Baron, T. Remy, J. Gascon, F. Kapteijn, *J. Am. Chem. Soc.* **2009**, *131*, 6326–6327.

[37] A. Stankiewicz, J. A. Moulijn, *Re-Engineering the Chemical Processing Plant: Process Intensification*, Taylor & Francis, London **2003**.

[38] W. D. Seider, J. D. Seader, D. R. Lewin, S. Widagdo, *Product and Process Design Principles: Synthesis, Analysis and Design*, John Wiley & Sons, New York **2008**.

[39] M. R. M. Abu-Zahra, J. P. M. Niederer, P. H. M. Feron, G. F. Versteeg, *Int. J. Greenhouse Gas Control* **2007**, *1*, 135–142.

[40] J. A. Moulijn, M. Makkee, A. E. van Diepen, *Chemical Process Technology*, John Wiley & Sons, New York **2013**.

[41] H. Devold, *Oil and Gas Production Handbook*, ABB AS Oslo, **2010**.

[42] G. Whitney, C. E. Behrens, T. Net, *Energy: Natural Gas: The Production and Use of Natural Gas, Natural Gas Imports and Exports*, EPAct Project, Liquefied Natural Gas (LNG) Import Terminals and Infrastructure Security, Thecapitol. Net, **2010**.

[43] S. W. Imbus, B. J. Katz, T. Urwongse, *Org. Geochem.* **1998**, *29*, 325–345.

[44] T. D. Lorenson, T. S. Collett, *Proc. Ocean Drill. Program* **2000**, 164.

[45] S. Couck, E. Gobechiya, C. E. A. Kirschhock, P. Serra-Crespo, J. Juan-Alcañiz, A. Martinez Joaristi, E. Stavitski, J. Gascon, F. Kapteijn, G. V. Baron, J. F. M. Denayer, *ChemSusChem* **2012**, *5*, 740–750.

[46] S. Peter, G. Baron, J. Gascon, F. Kapteijn, J. M. Denayer, *Adsorption* **2013**, 1–10.

[47] P. Serra-Crespo, R. Berger, W. Yang, J. Gascon, F. Kapteijn, *Chem. Eng. Sci.* **2015**, *124*, 96–108. DOI: 10.1016/j.ces.2014.10.028

[48] J. M. Douglas, *Conceptual Design of Chemical Processes*, McGraw-Hill, New York **1988**.

[49] J. Gascon, U. Aktay, M. D. Hernandez-Alonso, G. P. M. van Klink, F. Kapteijn, *J. Catal.* **2009**, *261*, 75–87.

[50] S. Couck, T. Remy, G. V. Baron, J. Gascon, F. Kapteijn, J. F. M. Denayer, *Phys. Chem. Chem. Phys.* **2010**, *12*, 9413–9418.

[51] P. Serra-Crespo, E. Gobechiya, E. V. Ramos-Fernandez, J. Juan-Alcañiz, A. Martinez-Joaristi, E. Stavitski, C. E. A. Kirschhock, J. A. Martens, F. Kapteijn, J. Gascon, *Langmuir* **2012**, *28*, 12916–12922.

[52] P. Serra-Crespo, A. Dikhtiarenko, E. Stavitski, J. Juan-Alcaniz, F. Kapteijn, F.-X. Coudert, J. Gascon, *CrystEngComm* **2015**, *17*, 276–280.

[53] P. Serra-Crespo, E. Stavitski, F. Kapteijn, J. Gascon, *RSC Adv.* **2012**, *2*, 5051–5053.

[54] J. M. Douglas, *AIChE J.* **1985**, *31*, 353–362.

[55] J. D. Seader, A. W. Westerberg, *AIChE J.* **1977**, *23*, 951–954.

[56] P. Serra-Crespo, R. Berger, W. Yang, J. Gascon, F. Kapteijn, *Chem. Eng. Sci.* **2015**, *124*, 96–108.

[57] C. Bach-Samario, N. Sundar, K. Verouden, T. Wezendonk, M. Zweemer, *A NH$_2$-MIL-53 Based CO$_2$ Removal Process – CDP 3387*, Delft University of Technology, **2012**.

[58] D. Domine, D. M. P. Guerin, *US Patent 3,242,645*, **1966**.

[59] J. E. Packer, J. Robertson, H. Wansbrough, *Chemical Processes in New Zealand*, Vol. II, New Zealand Institute of Chemistry, Auckland, **2008**.

[60] J. A. Moulijn, M. Makkee, A. van Diepen, *Chemical Process Technology*, John Wiley & Sons, New York **2001**.

[61] B. Crittenden, W. J. Thomas, *Adsorption Technology & Design*, Elsevier Science, New York **1998**.

[62] C. W. Skarstrom, *US Patent 2,944,627*, **1960**.

[63] C. A. Grande, *ISRN Chem. Eng.* **2012**, 13.

[64] Z. Liu, C. A. Grande, P. Li, J. Yu, A. E. Rodrigues, *Sep. Purif. Technol.* **2011**, *81*, 307–317.

[65] F. V. S. Lopes, C. A. Grande, A. E. Rodrigues, *Fuel* **2012**, *93*, 510–523.

[66] M. P. S. Santos, C. A. Grande, A. E. Rodrigues, *Ind. Eng. Chem. Res.* **2013**, *52*, 5445–5454.

[67] M. P. S. Santos, C. A. Grande, A. E. Rodrigues, *Chem. Eng. Sci.* **2011**, *66*, 1590–1599.

[68] M. P. S. Santos, C. A. Grande, A. E. Rodrigues, *Ind. Eng. Chem. Res.* **2010**, *50*, 974–985.

[69] S. J. Doong, R. T. Yang, *AIChE J.* **1987**, *33*, 1045–1049.

[70] E. Garcia-Perez, P. Serra-Crespo, S. Hamad, F. Kapteijn, J. Gascon, *Phys. Chem. Chem. Phys.* **2014**, *16*, 16060–16066.

[71] S. Ergun, *Chem. Eng. Prog.* **1952**, *48*, 89–94.

[72] S. Ergun, A. A. Orning, *Ind. Eng. Chem.* **1949**, *41*, 1179–1184.

[73] A. Freriks, *DACE Pricebookle*, Dutch Association of Cost Engineers, The Hague **2011**.

[74] www.theice.com/marketdata/reports/ReportCenter.shtml#report/168 (Accessed on May 15, 2014)

[75] www.ebn.nl/Actueel/Documents/ebn_focus_on_dutch_gas_2012.pdf (Accessed on May 15, 2014)

[76] L. D. Carter, *Enhanced Oil Recovery & CCS*, The U.S. Carbon Sequestration Council, **2011**.

[77] M. Peters, K. Timmerhaus, R. West, *Plant Design and Economics for Chemical Engineers*, McGraw-Hill Education, New York **2003**.

[78] J. Liu, P. K. Thallapally, B. P. McGrail, D. R. Brown, J. Liu, *Chem. Soc. Rev.* **2012**, *41*, 2308–2322.

[79] www.ceamag.com/index.php?option=com_content&view=article&id=31&Itemid=44&lang=en (Accessed on May 15, 2014)